

Structural phase transitions in Ruddlesden-Popper phases of strontium titanate: *ab initio* and inhomogeneous Ginzburg-Landau approaches

Jeehye Lee and Tomás A. Arias

Laboratory of Atomic and Solid State Physics, Cornell University, Ithaca, New York 14853

(Dated: August 20, 2010)

We present the first systematic *ab initio* study of anti-ferrodistortive (AFD) order in Ruddlesden-Popper (RP) phases of strontium titanate, $\text{Sr}_{1+n}\text{Ti}_n\text{O}_{3n+1}$, as a function of both compressive epitaxial strain and phase number n . We find all RP phases to exhibit AFD order under a significant range of strains, recovering the bulk AFD order as $\sim 1/n^2$. A Ginzburg-Landau Hamiltonian generalized to include inter-octahedral interactions reproduces our *ab initio* results well, opening a pathway to understanding other nanostructured perovskite systems.

PACS numbers: 73.21.Cd, 68.35.bg, 68.35.Rh

Superlattices originating from various oxide perovskites are of great interest due to their rich properties. As examples, Sr_2RuO_4 of the $n = 1$ Ruddlesden-Popper (RP) family exhibits unconventional superconductivity¹, ferroelectricity in multicomponent superlattices made of different perovskites (BaTiO_3 , SrTiO_3 and/or CaTiO_3) can be tuned by controlling the mixing ratio^{2,3}, and, recently, even a superconducting two-dimensional electron gas has been observed at the interface of the $\text{SrTiO}_3/\text{LaAlO}_3$ superlattice⁴.

The Ruddlesden-Popper series of structures, $\text{A}_{n+1}\text{B}_n\text{O}_{3n+1} = (\text{ABO}_3)_n(\text{AO})$ (or, “RP- n ”) for $n = 1, 2, \dots$, is the simplest prototype of such nano-ordered superlattices, consisting of a set of AO stacking fault planes interspersed regularly between every n layers of bulk perovskite octahedra⁵. The RP- n series most successfully synthesized to date is that of strontium titanate, with phases up to $n = 5$ reported to have been grown controllably with molecular beam epitaxy (MBE)⁶. The $n = \infty$ end member of the series, bulk SrTiO_3 , is also of great interest in its own right, with highly tunable properties such as strain-switchable ferroelectricity⁷, and even metallic and superconducting behavior under doping with oxygen vacancies^{8,9}.

Despite its technological and scientific potential, the RP- n series of strontium titanate remains relatively unexplored. The bulk material exhibits a rich strain-temperature structural phase diagram including both anti-ferrodistortive (AFD) and ferroelectric (FE) ordering and various combinations thereof¹⁰, with non-FE AFD order present at zero strain and temperature. In contrast, previous *ab initio* work has found there to be *no* AFD order at zero strain and temperature in the RP- n series for $n = 1, 2$, with the expected bulk-like order only occurring in $n = 3, 4, 5$ ^{11,12}. However, the associated phase transitions with strain, the underlying driving forces, the scaling of the behavior with n , and the nature of the large- n limit remains unexplored.

This work addresses the above open issues by employing the *ab initio* approach to study the AFD rotational transition as a function of both distance between stacking faults n and *epitaxial strain* (biaxial strain applied in the plane of the SrO stacking faults). Such epitaxial strain is

now accessible experimentally, with substrates available to provide a substantial range of strains to tune the material properties of strontium-titanate structures^{10,13,14}. For this initial study, we here focus on compressive strains, which favor AFD order with the rotation axis perpendicular to the stacking fault planes. This allows us to investigate the transition to bulk behavior with increasing n , while freeing us from having to consider the more complex configurations associated with the multiple, in-plane rotational axes favored by tensile strains.

Computational details – All *ab initio* calculations below employ the density-functional theory framework¹⁵ within the local-density approximation (LDA) and represent the ionic cores with norm-conserving Kleinman-Bylander pseudopotentials¹⁶. A plane-wave basis with a cutoff energy of 30 H expands the Kohn-Sham orbitals, and Monkhorst-Pack meshes¹⁷ of $2 \times 2 \times 2$ or $2 \times 2 \times 1$ (for RP- n structures of $n \leq 2$ or $n \geq 3$, respectively) sample the Brillouin zone. Finally, the resulting energy functional is minimized by the analytically continued conjugate gradient method¹⁸ within the DFT++ software¹⁹.

We employ supercells composed of two bulk regions, containing n strontium titanate bulk layers each, along with two extra SrO stacking fault layers. To properly represent the AFD order, each bulk layer contains two structural units of strontium titanate. To represent epitaxial strain, we fix the in-plane lattice parameter a and relax the out-of-plane lattice constant c . All calculations minimize the electronic wave functions to within 10 μH of the Born-Oppenheimer surface, the ionic coordinates until all forces on individual atoms $|\mathbf{F}|$ are less than 0.1 mH/B, and the out-of-plane strain until it is determined to within $\pm 0.2\%$ (1 H \approx 27.21 eV, 1 B \approx 0.0529 nm).

With the ultimate goal of comparing *ab initio* results to experiments on epitaxially strained thin films, we define epitaxial strains as $\epsilon \equiv (a - a_B)/a_B$, where $a_B = 3.8376 \text{ \AA}$ is the equilibrium lattice constant for cubic (non-rotated) bulk SrTiO_3 within our computational framework. We find that small- n phases under sufficiently low compressive strains either exhibit AFD order with an out-of-plane rotation axis or remain non-ordered (centrosymmetric). To obtain reliable transition points for low- n phases and to extract information about

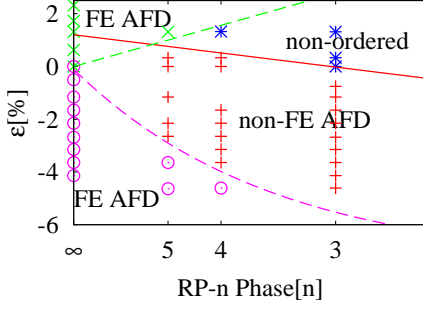


FIG. 1: (Color online) Structural phase diagram of $\text{Sr}_{n+1}\text{Ti}_n\text{O}_{3n+1}$ as a function of epitaxial strain and n : in-plane FE AFD order (\times), out-of-plane FE AFD order (\circ), out-of-plane non-FE AFD order ($+$), non-ordered ($*$), non-FE AFD to non-ordered phase boundary studied in the text (solid line), additional phase boundaries (dashed lines).

bulk SrTiO_3 that can be connected directly to our results at low n , we sometimes enter regions of phase space where the material exhibits other instabilities. Figure 1 summarizes the phase space we considered and the phases we found in each region. Under sufficiently high compressive or tensile strains, AFD and FE orders coexist in the large- n phases with the order parameters oriented along either the out-of- or in-plane directions, respectively, just as in bulk strontium titanate¹⁰.

Concerned here only with the transition between the out-of-plane non-FE AFD phase and the non-ordered phase, for the calculations below, we suppress FE order and in-plane AFD order by imposing both C_2 and mirror symmetry about the out-of-plane direction. Figure 1 shows that, for $n \leq 4$ and low strains, the ground-state phases are free of these suppressed orders, so these symmetry restriction *in no way* affect our conclusions for the $n \leq 4$ phases. For the $n \geq 5$ phases, the in-plane rotated order will likely become more thermodynamically stable near the phase-transition point of interest to us. Thus, for large n , the rotated phases which we study may be only metastable near the transition point. Because we here are concerned with the nature of the non-FE AFD to non-ordered phase boundary and how the spacing n between stacking faults affect this transition, the imposition of the above symmetry restrictions again does not affect the central conclusions below.

Sr₂TiO₄, $n = 1$ phase – As a first look at the AFD phase transition under strain, we begin by noting that, by the symmetries of the $00c^-$ AFD ordering in the Glazer notation²⁰, a single rotation angle θ serves to define the state of rotation for each layer of octahedra. In a very simple picture in which the rotations in all layers in each bulk region are the same (as is the case for the $n = 1, 2$ phases), we would have a single order parameter and the usual Ginzburg-Landau form for the free energy,

$$F(\theta) = \frac{1}{2}A\theta^4 + \alpha(\epsilon - \epsilon_c)\theta^2 + F_0, \quad (1)$$

where both A and α are positive, and ϵ_c is the criti-

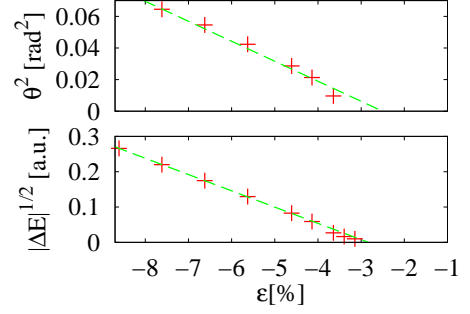


FIG. 2: (Color online) Square of rotational order parameter, θ^2 , versus epitaxial strain ϵ (upper panel); square-root of transition energy, $\sqrt{\Delta E}$, versus epitaxial strain ϵ (lower panel): *ab initio* results (crosses), linear fits (dashed lines).

cal strain of the transition, with the well-known solution that the ordered phase obtains for $\epsilon < \epsilon_c$, with a nonzero rotation angle $\theta^2(\epsilon) = \alpha(\epsilon_c - \epsilon)/A$ and an energy difference relative to the centrosymmetric state ($\theta = 0$) of $\sqrt{\Delta E(\epsilon)} = \alpha(\epsilon_c - \epsilon)/\sqrt{2A}$. Thus, the *square* of rotation angle and the *square-root* of the energy difference should both vanish linearly as ϵ approaches ϵ_c from below. (Here and below we regard compressive strains as $\epsilon < 0$.)

Figure 2 shows that our full *ab initio* results for the $n = 1$ RP phase exhibit quite clearly these classic signatures of a second-order phase transition. The extrapolated values for the critical strain from the two observables, θ^2 and $\sqrt{\Delta E}$, are in surprisingly good agreement for such a simple model, -2.2% and -2.8%, respectively. In either case, it is clear that the critical strain is significantly below zero, consistent with the lack of observation of AFD rotational order in the $n = 1$ phase near zero strain in previous *ab initio* work¹¹. As we now show, the critical strain passes through zero and becomes positive with increasing n , eventually approaching a value associated with the bulk material.

Sr_{n+1}Ti_nO_{3n+1}, $n > 1$ phase – For $n > 1$, multiple perovskite layers exist between faults and different rotation angles become possible for each layer (except for the $n = 2$ phase where the two layers are identical by symmetry). The upper panel of Figure 3 displays the rotation angles in each layer for the $n = 5$ phase at zero strain. These data exhibit the general trend in all of our data, namely that the rotation angles are smaller near the SrO stacking faults and approach the expected bulk value toward the center of the bulk regions. Associated with the reduced rotation angle at the interface, we find an enhanced stretching of the octahedra neighboring the stacking faults resulting in rumpling of the SrO layers. We also find off-center motion of the titanium ions of these boundary octahedra toward the fault layers, so that each region of bulk material, and thus the entire structure, exhibits no net ionic electric dipole moment. This suggests that the structure near the SrO stacking faults is such that the boundary octahedra prefer stretching and formation of a ionic electric dipole moment over

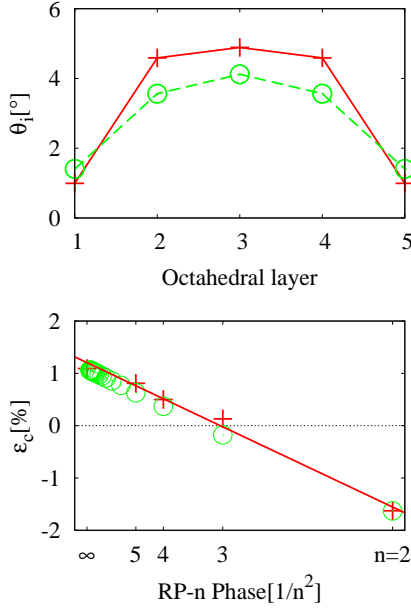


FIG. 3: (Color online) *Ab initio* (+) and Ginzburg-Landau model (o) results for layer-dependent rotation angles θ_i versus layer position for the $n = 5$ phase at $\epsilon = 0.0\%$ (upper panel), and critical strain ϵ_c versus *inverse-square* of RP phase number n (lower panel). Lines in upper panel are guides to the eyes; solid line in lower panel is best fit to *ab initio* data.

rotation as a way to relieve compressive stress, ultimately suppressing the rotational instability near the faults.

To locate the AFD transition, for the order parameter θ , we take the rotation angle of the central one or two (if n is odd or even, respectively) perovskite layers, and extrapolate the linear behavior of θ^2 (which shows less numerical scatter than that for $\sqrt{\Delta E}$), identifying the horizontal intercept as the critical strain²¹. The lower panel of Figure 3 displays the resulting critical strains for $n \geq 2$ as a function of $1/n^2$. With increasing n , the critical strain steadily increases toward the bulk value as the RP- n phases become more like bulk. The critical strains are *negative* for $n = 1, 2$ and *positive* for $n \geq 3$, consistent with and explaining the previous *ab initio* observations^{11,12} that only $n \geq 3$ phases exhibit AFD order when grown on a bulk SrTiO₃ substrate ($\epsilon = 0\%$). Finally, the clear linear behavior in the plot indicates that the critical strain approaches the bulk value as $1/n^2$.

To explore the origin of the above behaviors, we generalize the above Ginzburg-Landau free-energy model to inhomogeneous systems by including both inter-octahedral interactions and a spatially-dependent tendency toward rotational instability,

$$F(\{\theta_i\}) = \sum_i \left\{ \frac{1}{2} A \theta_i^4 + \alpha (\epsilon - \epsilon_i) \theta_i^2 + \beta (\theta_i + \theta_{i-1})^2 \right\}, \quad (2)$$

where θ_i is the octahedral rotation angle of the i -th layer, A and α are defined as above (Eq. 1), ϵ_i represents an effective critical strain for the i -th layer, and the third,

inter-layer term imposes the alternating sign ordering of θ_i associated with the Glazer $00c^-$ order of the material. To reflect the lessened tendency towards rotation at the interfaces, ϵ_i should have more negative values near the stacking faults, eventually approaching the critical value for the bulk material $\epsilon_c(n = \infty)$ in the center of the bulk regions. In this initial work, we take ϵ_i to be the bulk value $\epsilon_c(\infty)$ for all layers i except those neighboring the stacking faults, for which we will take a different value, $\epsilon_i = \tilde{\epsilon}$, to be determined below. The standard stability analysis for this free energy is that there will be a second-order phase transition when the Hessian, evaluated at $\theta_i = 0$ for all i , ceases to be positive definite.

To begin our analysis of the above free-energy form, we consider the approach to the bulk behavior. For sufficiently large n , one can take the continuum limit, and the Hessian becomes $H = (\epsilon - \epsilon_c(\infty))\theta(x) - (d^2\beta/\alpha)\partial^2\theta/\partial x^2$, where ϵ retains its meaning as the applied strain, d is the distance between adjacent layers and x is the position within the bulk region along the c -axis. Here, the layer-dependent rotation angle $(-1)^i\theta_i$ has now become the smooth function $\theta(x)$. Finally, in passing to the continuum limit, there is a boundary condition associated with the interfaces, which for our simple model is $(\epsilon_c(\infty) - \tilde{\epsilon})\theta(x) = (d\beta/\alpha)\partial\theta/\partial x$, for $x = 0, nd$. The critical point where this continuum Hessian ceases to be positive definite corresponds to the lowest eigenvalue of the standard one-dimensional particle-in-a-box problem of quantum mechanics with a modified boundary condition. The resulting critical strain is $\epsilon_c = \epsilon_c(\infty) - (\beta q^2)/(\alpha n^2)$, where q satisfies the transcendental equation $\tan(q/2) = \alpha n (\epsilon_c(\infty) - \tilde{\epsilon})/(\beta q)$, whose solution approaches a constant, $q \rightarrow \pi$, for large n . The continuum limit thus reproduces exactly the $1/n^2$ approach to the bulk value observed in the *ab initio* data. The slope γ observed in the *ab initio* data can now be identified as a combination of parameters from the Ginzburg-Landau Hamiltonian, namely $\gamma = (\beta/\alpha)\pi^2$.

Using the observed slope in the *ab initio* data as well as data from the bulk and $n = 2$ phases, we now determine completely the parameters in the Ginzburg-Landau model. In the bulk phase, the last term of Eq. 2 vanishes due to the AFD order, and the analysis becomes identical to that for $n = 1$ phase, in which A , α and $\epsilon_c(\infty)$ can all be determined from the linear fits to the θ^2 and $\sqrt{\Delta E}$ versus ϵ data. When $n = 2$, by symmetry, the Hamiltonian again assumes a form of Eq. 1, but with $\tilde{\epsilon}$ instead of $\epsilon_c(\infty)$, so that we directly read off $\tilde{\epsilon} = \epsilon_c(n = 2)$. The final parameter remaining is β , which we determine from the above result for γ in terms of β and α , taking γ from the slope of the best-fit line to the *ab initio* data (solid line, lower panel of Figure 3).

The open circles in the lower panel of Figure 3 represent the critical strains from eigenvalues of the above Hessian for inhomogeneous systems, with parameters extracted from the *ab initio* results as above. The clear linear behavior confirms our analytic prediction that the critical strain in the model approaches the bulk value as

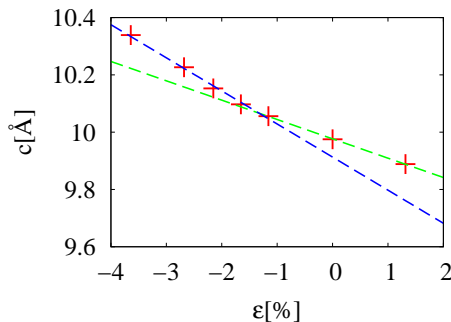


FIG. 4: (Color online) Out-of-plane lattice constant versus the biaxial strain ϵ : *ab initio* results (+), linear fits to data on either side of the transition (dashed lines).

$1/n^2$. The upper panel of Figure 3 presents an even more compelling case for the model free energy. It compares *ab initio* and model-Hamiltonian results for a quantity not included in the parameter fitting at all, the layer-dependent rotation angles θ_i for the $n = 5$ RP- n phase at $\epsilon = 0\%$ strain. The agreement is impressive considering the simplicity of the model and the fact that the model is not fit to these quantities.

Experimental signatures — In terms of an experimentally observable signature of this transition, we find that, associated with the rotational ordering, there is a significant expansion of the out-of-plane lattice constant c , by an amount which should be readily detectable with x-ray techniques. Figure 4 shows the lattice constant c of the $n = 2$ phase as a function of ϵ through the AFD transition point. The transition is clearly evident where the slope of the curve changes substantially between $\epsilon = -1\%$ and -2% strain. The lattice constant c for the AFD phase is significantly larger ($> 0.6\%$ for strains $\epsilon < -2.6\%$, about 1% strain beyond the transition) than the extrapolated value from the non-rotated phase. A perhaps more practical approach is to grow various members of the RP-

n series on substrates of *fixed* epitaxial strain ϵ and to observe the dependence $c(n)$ of the out-of-plane lattice constant as a function of n , looking again for a kink at the transition point. We stress that the numerical values given here apply specifically to zero temperature.

Conclusion — This work presents a detailed *ab initio* study of the effects of strain on the rotational instability in the Ruddlesden-Popper series in strontium titanate for $n = 1, \dots, 5$. We find a similar second-order structural phase transition to what is seen in bulk strontium titanate, but with a critical point displaced by $\sim 1/n^2$ from the bulk value. The key microscopic mechanism for the n -dependence is the interplay of the local AFD coupling between neighboring octahedra layers with a depression of the rotational instability for octahedra immediately neighboring the SrO stacking faults. It appears that the depression is associated with the extra freedom which the neighboring octahedra have to distort by formation of local ionic electric dipole moments and by rumpling of the extra SrO layers. A simple Ginzburg-Landau free-energy expression generalized for inhomogeneous systems by inclusion of nearest-neighbor inter-octahedral interactions captures the essential features of the *ab initio* results for the n -dependence of the transition. Despite its simplicity, this free-energy expression gives reasonable predictions even for quantities to which it is not fit, such as the distribution of rotation angles in the bulk regions of the RP phase. This success suggests that inclusion of inter-octahedral interactions into more general bulk Hamiltonians, particularly those with ferroelectric degrees of freedom, will be a fruitful direction to pursue in future studies of nano-structured and superlattice perovskite materials.

This work was supported by the Cornell Center for Materials Research (CCMR) under the NSF MRSEC program (DMR-0520404). The authors are grateful to Craig Fennie for many fruitful discussions.

-
- ¹ K. Ishida et al., Nature **396**, 658 (1998).
 - ² S. M. Nakhmanson, K. M. Rabe, and D. Vanderbilt, Phys. Rev. B **73**, 060101(R) (2006).
 - ³ K. Johnston, X. Huang, J. B. Neaton, and K. M. Rabe, Phys. Rev. B **71**, 100103(R) (2005).
 - ⁴ M. Basletic et al., Nature Material **7**, 621 (2008).
 - ⁵ S. N. Ruddlesden and P. Popper, Acta Cryst. **10**, 538 (1957).
 - ⁶ W. Tian, X. Q. Pan, J. H. Haeni, and D. G. Schlom, J. Mater. Res. **16**, 2013 (2001).
 - ⁷ J. H. Haeni et al., Nature **430**, 758 (2004).
 - ⁸ H. P. R. Frederikse and W. R. Hosler, Physical Review **158**, 775 (1967).
 - ⁹ C. S. Koonce et al., Physical Review **163**, 380 (1967).
 - ¹⁰ Y. L. Li et al., Phys. Rev. B **73**, 184112 (2006).
 - ¹¹ C. Fennie and K. Rabe, Phys. Rev. B **68**, 184111 (2003).
 - ¹² S. M. Nakhmanson, Phys. Rev. B **78**, 064107 (2008).
 - ¹³ N. D. Orloff et al., Appl. Phys. Lett. **94**, 042908 (2009).
 - ¹⁴ M. P. Warusawithana et al., Science **324**, 367 (2009).
 - ¹⁵ M. C. Payne et al., Rev. Mod. Phys. **64**, 1045 (1992).
 - ¹⁶ L. Kleinman and D. M. Bylander, Phys. Rev. Lett. **48**, 1425 (1982).
 - ¹⁷ H. J. Monkhorst and J. Pack, Phys. Rev. B **13**, 5188 (1976).
 - ¹⁸ T. A. Arias, M. C. Payne, and J. D. Joannopoulos, Phys. Rev. Lett. **69**, 1077 (1992).
 - ¹⁹ S. Ismail-Beige and T. A. Arias, Computer Physics Communications **128**, 1 (2000).
 - ²⁰ A. M. Glazer, Acta Cryst. **B28**, 3384 (1972).
 - ²¹ The LDA overbinding error may lead to an uncertainty in transition points as the AFD rotational instability is known to be overestimated.